JGR Biogeosciences

RESEARCH ARTICLE
10.1029/2022JG006891

Key Points:

- Variation in hydrochemistry across tundra aquatic environments was more strongly coupled to physiographic factors than to wildfire effects
- Wildfire generally reduced dissolved organic carbon (DOC) and CO_2, and enhanced ion mobility and nitrogen cycling, but effects varied
- Wildfire effects on some hydrochemical constituents persisted beyond 3 years (e.g., DOC, CO_2) and were brief for others (conductivity)

Supporting Information:

Supporting Information may be found in the online version of this article.

Correspondence to:

S. Zolkos,
sgzolkos@gmail.com

Citation:

Zolkos, S., MacDonald, E., Hung, J. K. Y., Schade, J. D., Ludwig, S., Mann, P. J., et al. (2022). Physiographic controls and wildfire effects on aquatic biogeochemistry in tundra of the Yukon-Kuskokwim Delta, Alaska. *Journal of Geophysical Research: Biogeosciences*, *127*, e2022JG006891. https://doi.org/10.1029/2022JG006891

Received 17 MAR 2022
Accepted 6 JUN 2022

Physiographic Controls and Wildfire Effects on Aquatic Biogeochemistry in Tundra of the Yukon-Kuskokwim Delta, Alaska

Scott Zolkos[1], Erin MacDonald[1], Jacqueline K. Y. Hung[1], John D. Schade[1], Sarah Ludwig[1,2], Paul J. Mann[3], Rachael Treharne[1], and Susan Natali[1]

[1]Woodwell Climate Research Center, Falmouth, MA, USA, [2]Department of Earth and Environmental Sciences, Columbia University, New York, NY, USA, [3]Department of Geography and Environmental Sciences, Northumbria University, Newcastle Upon Tyne, UK

Abstract Northern high-latitude deltas are hotspots of biogeochemical processing, terrestrial-aquatic connectivity, and, in Alaska's Yukon-Kuskokwim Delta (YKD), tundra wildfire. Yet, wildfire effects on aquatic biogeochemistry remain understudied in northern delta regions, thus limiting a more comprehensive understanding of high latitude biogeochemical cycles. In this study, we assess wildfire impacts on summertime aquatic biogeochemistry in YKD tundra using a multi-year (2015–2019) data set of water chemistry measurements ($n = 406$) from five aquatic environments: peat plateau ponds, fen ponds, fen channels, lakes, and streams. We aimed to (a) characterize variation in hydrochemistry among aquatic environments; (b) determine wildfire effects on hydrochemistry; and (c) assess post-fire multi-year patterns in hydrochemistry in lakes (lower terrestrial-freshwater connectivity) and fen ponds (higher connectivity). Variation in hydrochemistry among environments was more strongly associated with watershed characteristics (e.g., terrestrial-aquatic connectivity) than wildfire. However, certain hydrochemical constituents showed consistent wildfire effects. Decreases in dissolved organic carbon (DOC) and CO_2, and increases in pH, specific conductance, NH_4^+, and NO_3^- indicate that, by combusting soil organic matter, wildfire reduces organics available for hydrologic transport and microbial respiration, and mobilizes nitrogen into freshwaters. Multi-year post-fire variation in specific conductance, DOC, and CO_2 in lakes and fen ponds suggest that watershed characteristics underlie ecosystem response and recovery to wildfire in the YKD. Together, these results indicate that increasing tundra wildfire occurrence at northern high latitudes could drive multi-year shifts toward stronger aquatic inorganic nutrient cycling, and that variation in terrain characteristics is likely to underlie wildfire effects on aquatic ecosystems across broader scales.

Plain Language Summary Warming at northern high latitudes is expected to increase wildfire activity, permafrost thaw, and hydrologic connectivity. Yet, contrasting evidence for wildfire effects on aquatic biogeochemistry hinders a more concrete understanding of potential future changes to northern ecosystems, especially in delta environments, where land-freshwater linkages are strong. To address this, we made ~400 measurements of hydrochemistry within the Yukon-Kuskokwim Delta, Alaska, following high wildfire activity in 2015. Variation in hydrochemistry among five aquatic environments—peat plateau ponds, fen ponds, fen channels, lakes, and streams—was more strongly associated with watershed characteristics (e.g., land-freshwater linkages) than wildfire. However, wildfire consistently affected some parameters. For instance, dissolved organic carbon and CO_2 were lower in burned watersheds, likely from combustion of organic matter, whereas, pH, specific conductance, and nitrogen were higher, reflecting solute release from combusted organics. Multi-year measurements (2015–2019) allowed us to assess post-fire variation in hydrochemistry among lakes and fen ponds, and indicate that ecosystem response and recovery to wildfire depend on watershed characteristics. Results indicate that increasing tundra wildfire at northern high latitudes could drive multi-year shifts toward stronger aquatic inorganic nutrient cycling. Across broader spatiotemporal scales, variation in terrain characteristics is likely to underlie wildfire effects on aquatic ecosystems.

1. Introduction

Biogeochemical cycling is shaped by varied physiographic conditions across landscapes, and changes to these landscapes are reflected in aquatic chemistry (Drake et al., 2018; Toohey et al., 2016). This is particularly evident

at northern high latitudes, where large stores of nutrients in permafrost environments (Hugelius et al., 2020) are increasingly susceptible to lateral transfer into aquatic environments due to climate warming, permafrost thaw, and wildfire (Frey & McClelland, 2009; Shogren et al., 2019). While aquatic biogeochemical cycles are strongly coupled to regional variation in physiographic factors including watershed elevation and slope (Connolly et al., 2018), vegetation productivity (Hutchins et al., 2019), and hydrology (Striegl et al., 2007), contrasting evidence for wildfire effects on aquatic biogeochemistry (Larouche et al., 2015; Rodríguez-Cardona et al., 2020) hinders a more concrete understanding of potential future changes to northern ecosystems.

As climate warming and wildfire regimes intensify at northern high latitudes (Kasischke et al., 2010; Rocha et al., 2012), changes in surface water chemistry are hypothesized to be a key indicator of aquatic and terrestrial ecosystem response to environmental change (Hutchins et al., 2020; Larouche et al., 2015; Rodríguez-Cardona et al., 2020). The interconnected nature of vegetation, soils, and hydrology allow for wildfire effects to cascade beyond the land surface because wildfire changes the composition of aboveground vegetation (Bret-Harte et al., 2013; Frost et al., 2020), deepens the active layer (Holloway et al., 2020), and alters subsurface hydrology (Ackley et al., 2021). In landscapes with strong terrestrial-aquatic connectivity, which is often the case in smaller watersheds, wildfire can decrease nutrient and organic matter in downstream environments (Abbott et al., 2021; Rodríguez-Cardona et al., 2020). Although wildfire effects are not likely to be uniform across landscapes with different physiographic conditions (e.g., hydrology, vegetation cover, land-freshwater connectivity), the relative importance of physiographic conditions versus wildfire on aquatic biogeochemistry is important to constrain for understanding potential future trajectories of northern ecosystem change.

Northern deltas are hotspots of ecological diversity, nutrient storage, and biogeochemical processing, and are characterized by strong land-freshwater linkages. The Yukon-Kuskokwim Delta (YKD) in southwestern Alaska is primarily coastal lowlands with interior tundra underlain by sporadic and discontinuous permafrost (Brown et al., 2002). Wildfire activity has greatly affected the YKD landscape, especially in recent years. In 2015 alone, wildfires burned over 420 km^2 in YKD uplands (AICC, 2019). Lacustrine sedimentary records indicate that intervals of more frequent and intense wildfire during the Holocene were instigated by warmer air temperatures (Sae-Lim et al., 2019). Although wildfire is certain to affect aquatic ecosystems in the YKD, the magnitude and duration of the effects are unknown and challenging to estimate solely based on findings elsewhere because of large regional variation. Additionally, multi-year post-fire effects on aquatic chemistry are seldom studied, in part due to the logistical challenge presented by the stochastic nature of wildfire occurrence (Burd et al., 2018; Hutchins et al., 2020; Koch et al., 2014; Larouche et al., 2015; Rodríguez-Cardona et al., 2020).

Here, we make a first assessment of physiographic controls and wildfire effects on aquatic biogeochemistry in the YKD using a multi-year (2015–2019) data set of samples ($n \sim 400$) collected among five aquatic environments: peat plateau ponds, fen ponds, fen channels, lakes, and streams (Figure 1). Watersheds of these aquatic environments vary with respect to area, elevation, vegetation, and hydrology, allowing us to determine the degree to which landscape factors control hydrochemistry, and how their effects interact with recent wildfire. Using surface water and pore water chemistry data collected over 5 years following wildfire, we sought to address the question: what is the influence of recent wildfire (2015) on aquatic biogeochemistry in YKD tundra? Our objectives were to: (a) determine wildfire effects on hydrochemistry among YKD aquatic environments; (b) compare wildfire effects on carbon and nutrient cycling in aquatic environments with relatively lower connectivity (lakes) and higher connectivity (fen ponds) with the surrounding landscape; and (c) characterize multi-year post-fire patterns in aquatic biogeochemistry.

2. Methods

2.1. Study Area

Sampling occurred in the Izaviknek and Kingaglia Uplands, a 3,900 km^2 region situated 10–65 m above sea level and underlain by discontinuous permafrost (Frost et al., 2020). This tundra landscape is characterized by peatland plateaus and by interconnected lakes, fens, and streams. Terrestrial vegetation on unburned peat plateaus is dominated by lichen and low-lying shrubs, while vegetation in aquatic systems is typically dominated by *Sphagnum* and graminoid *spp.* (Frost et al., 2020). At the Bethel airport 75 km southeast of the study area, the mean annual and July air temperatures from 2015 to 2019 were 1.8°C and 14.7°C, respectively (NOAA, 2020). Mean annual and July precipitation were 536 and 62.1 mm, respectively. Wildfires in the YKD typically occur

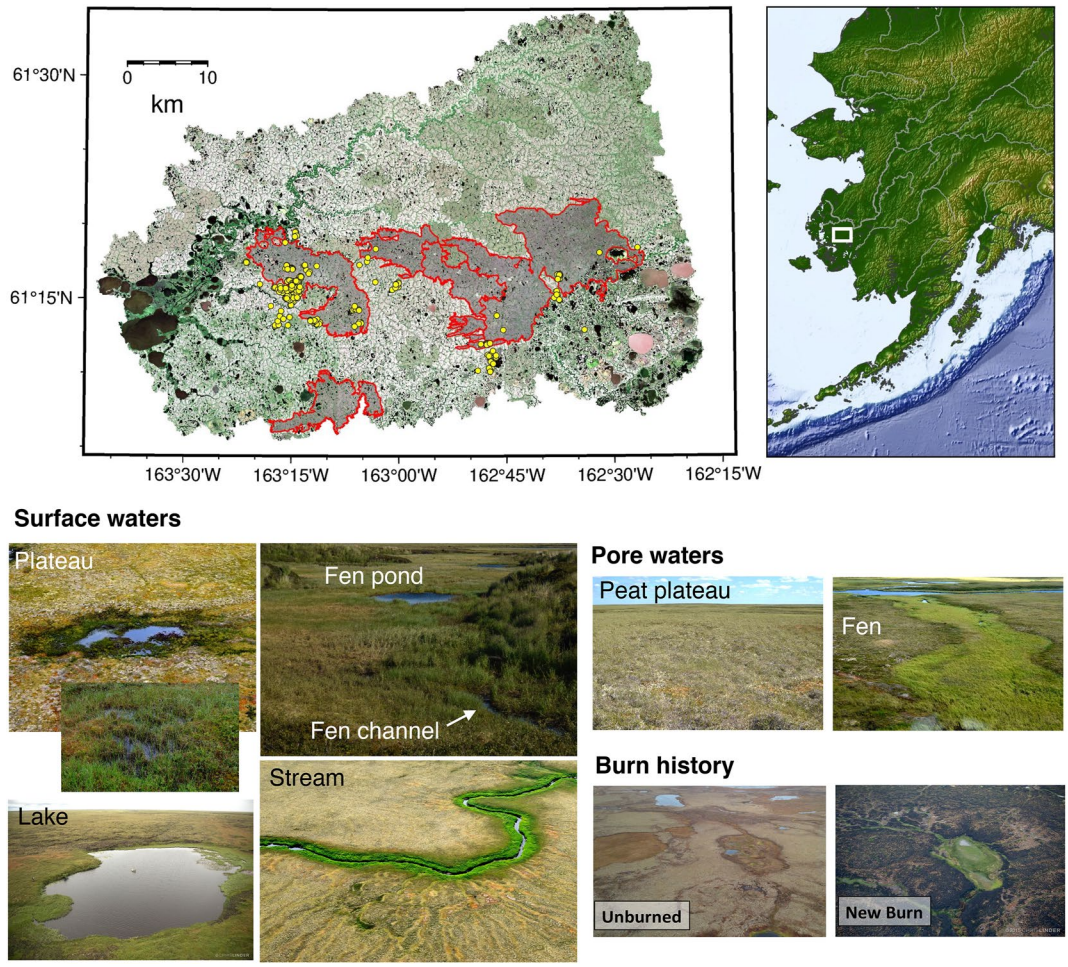

Figure 1. Top left: map of sampling sites (yellow points) within the study area. Red polygons outline perimeters of wildfires during 2015. Map created using Generic Mapping Tools (Wessel et al., 2019). Top right: location of study area within Alaska (white box). Terrain relief data obtained from Tozer et al. (2019). Bottom: aquatic environments within the Yukon-Kuskokwim Delta that were sampled for (a) surface waters and (b) pore waters across terrain that was (c) unburned or burned in 2015. Photographs are in true color and all were made by Chris Linder Photography.

during the thaw season (late spring through late summer), and were abundant in 2015 due to anomalously high thaw-season air temperatures and lightning strikes (Veraverbeke et al., 2017). Although YKD tundra wildfires are relatively low intensity due to limited fuel availability, they often combust the widespread surficial lichen and decrease surface organic soil layer thickness (Frost et al., 2020).

Sampling occurred at 406 sites within 50 km of 61.263°N, 163.246°W during summertime (June–September) from 2015 to 2019 (Figure 1; Table S1 in Supporting Information S1). Surface water samples were collected at 343 sites and pore water samples at 63 sites. Most (nearly 70%) of samples were collected in July in order to focus on characterizing patterns in hydrochemistry among aquatic environments, rather than revisiting specific sites multiple times during the summer to assess potential changes in hydrochemistry associated with seasonal thaw. We identified five primary aquatic and wetland environments that differ in landscape position, vegetation, hydrologic regimes, and connectivity with the landscape: peat plateau ponds (henceforth, plateau ponds) (n = 31), fen ponds (n = 21), lakes (n = 159), fen channels (n = 179), and streams (n = 16) (Figure 1). Plateau ponds were characterized by relatively small (≤10 m diameter), shallow (<0.5 m), and hydrologically isolated and relatively ephemeral bodies of water, some with muddy sediments or dead moss underlying the water column. Plateau ponds did not have a peripheral bank, rarely contained submerged aquatic vegetation, and were likely to dry and recede between rain events. In some cases, these surface waters formed only under wet conditions, when the active layer was saturated. Fens are thought to have a strong connection to the terrestrial environment and are

dominated by *Sphagnum spp.*, other hydrophilic mosses, and graminoids, with large willow shrubs occasionally present. Fen ponds were generally small and connected hydrologically by fen channels. Lakes in the YKD were typically 1–3 m deep, had 1–3 m high banks, and ranged in size from 10 m to >1 km in diameter. Lakes were often relatively turbid and some had emergent aquatic vegetation. Streams had clearly defined banks and channels, riparian zones with deciduous shrubs, with varying amounts of submerged aquatic vegetation.

2.2. Surface and Pore Water Sample Collection

Water sampling targeted areas that were either burned in 2015 or unburned, to assess the immediate post-fire response of tundra aquatic ecosystems to wildfire. At all surface water sampling sites, water temperature, specific conductance (henceforth, conductivity), pH, and dissolved oxygen (D.O.) were measured using a pre-calibrated Professional-Plus water quality meter (Yellow Springs Instruments). Water samples for dissolved organic carbon (DOC), total dissolved nitrogen (TDN), ammonium (NH_4^+), nitrate (NO_3^-), phosphate (PO_4^{3-}), and optical properties of chromophoric dissolved organic matter (CDOM) were collected in sample-rinsed polypropylene syringes and filtered (0.7 µm glass fiber filter, Whatman) into acid-washed, sample-rinsed high density polyethylene bottles. Filtrate was stored frozen until analysis in the laboratory. Water for dissolved inorganic carbon (DIC) concentration and stable isotopes (δ^{13}C-DIC) and CH_4 stable isotopes (δ^{13}C-CH_4) was injected into sealed glass vials; samples for δ^{13}C-DIC were acidified with 100 µl of H_3PO_4. Water for stable isotopes of water (δ^2H-H_2O, δ^{18}O-H_2O) was filtered directly into glass vials without headspace or air bubbles. Samples for DIC and H_2O stable isotopes were stored cool (4°C) and dark prior to analysis.

Dissolved CO_2 and CH_4 in water were collected in triplicate using the headspace equilibration method (Hesslein et al., 1991). 30 mL of water sample and 30 mL of atmosphere was shaken vigorously for 1 minute within a sealed polypropylene syringe. The equilibrated headspace gas was injected into a pre-evacuated glass vial sealed with a butyl septum to achieve positive pressure and stored dark and at ambient temperature until analysis. Water and air temperature and atmosphere pressure were recorded to correct later calculations of CO_2 and CH_4 concentration.

CO_2 and CH_4 efflux from surface waters to the atmosphere were measured as the change in gas concentration within the headspace of a stationary floating chamber. Continuous measurements of CO_2 and CH_4 concentrations within the flux chamber headspace were collected for up to 20 minutes using a portable greenhouse gas analyzer (Ultraportable Greenhouse Gas Analyzer, Los Gatos Research). Fluxes were calculated as the change in headspace gas concentrations during the sampling interval.

Pore water was collected from wells or sippers and processed in the same fashion as surface water samples. Wells made of polyvinyl chloride tubing were installed into the organic layer using a hand drill and undisturbed for 24 hr prior to sampling to minimize potential disturbance effects by installation. Pore water samples were collected using a polypropylene syringe or, when required for deeper wells, a peristaltic pump (Geopump) with silicone tubing (Masterflex). Owing to potential disturbance from pumping action on dissolved gases, CO_2 and CH_4 were not collected when well water samples were collected using a peristaltic pump. Sippers were installed into the organic layer and pore water was extracted at <30 mL/min via a syringe connected to tubing.

2.3. Laboratory Analyses

DOC and TDN were analyzed by high-temperature oxidation followed by infrared detection of CO_2 and chemiluminescent detection of NO (Shimadzu TOC-V/TNM-1) at the Woodwell Climate Research Center (Woodwell) Environmental Chemistry Laboratory (ECL). DOC and TDN concentrations were calculated as the mean of three to five injections and the coefficient of variance was <2%. MilliQ DI water blanks, standard reference material, and in-house references for carbon (10 ppm, caffeine) and nitrogen (1 ppm, NH_4^+) were routinely measured as quality checks during each run.

Inorganic nutrients (NH_4^+, NO_3^-, PO_4^{3-}) were measured on an Astoria Analyzer at the Woodwell ECL following established protocols (U.S. Environmental Protection Agency, 1984). Dissolved organic nitrogen was calculated as the difference between TDN and dissolved inorganic nitrogen (DIN = $\Sigma[NH_4^+, NO_3^-, NO_2^-]$).

We calculated specific UV absorbance at 254 nm ($SUVA_{254}$) to characterize dissolved organic matter aromaticity, which is an indicator of reactivity (Weishaar et al., 2003). Optical absorbance of CDOM in the UV-visible range (200–800 nm) was measured in duplicate at 20°C using a Shimadzu dual-beam UV-1800 spectrophotometer at

the Woodwell ECL within 4 weeks of collection. MilliQ water blanks were measured at the beginning and end of each run to monitor for instrument drift, and mean absorbance from 700 to 800 nm was used to correct each sample for offset from scattering (Stubbins et al., 2017). Corrected spectra were used to calculate $SUVA_{254}$ as the decadic absorption at 254 nm coefficient divided by DOC concentration (Weishaar et al., 2003). $SUVA_{254}$ positively correlates with dissolved organic matter aromaticity; lower values are associated with relatively more labile organic matter in northern aquatic environments (Littlefair & Tank, 2018; Wickland et al., 2012). Slope ratios (S_R) were calculated using log-linear fits of corrected absorbance spectra from 275 to 295 and 350–400 nm (Helms et al., 2008). In northern freshwaters, higher S_R values are associated with organic matter with a lower molecular weight and therefore may be relatively more biolabile and/or photodegraded (Helms et al., 2008; Littlefair & Tank, 2018; Ward & Cory, 2016). We used $SUVA_{254}$ and S_R to evaluate relative organic carbon reactivity in aquatic environments.

Dissolved CO_2 and CH_4 were analyzed by a gas chromatograph equipped with a flame ionization detector at the Woodwell ECL (GC-2014, Shimadzu Scientific Instruments). Stable carbon isotope values, which reflect fractionation associated with abiotic and biotic processes (Kendall et al., 2014), were used to infer potential carbon sources. Stable isotopes of DIC, CH_4, and H_2O were analyzed at the Northumbria University Cold and Paleo-Environment Group Laboratory. δ^{13}C-DIC and δ^{13}C-CH_4 were measured by isotope ratio mass-spectrometry (Thermo Delta V Advantage interfaced to a Gas Bench II) and δ^{18}O-H_2O and δ^{2}H-H_2O by cavity ringdown spectroscopy (IWA45-EP, Los Gatos Research). Values are reported in permil (‰) relative to Pee-Dee Belemnite (VPDB). d-excess ($\delta^{2}H - 8 \times \delta^{18}O$), a metric for disequilibrium isotope effects (Jasechko, 2019), was used to quantify deviation of surface water samples from the global meteoric water line (GMWL) (Kendall et al., 2014). Deviation in d-excess from the GMWL (d-excess = 8‰) reflects isotopic fractionation associated with hydroclimatic processes, providing useful inference on variation in water sources (Jasechko, 2019). For instance, lower d-excess values indicate greater effects from evaporation (Hutchins et al., 2019; Tondu et al., 2013; Turner et al., 2014).

2.4. Geospatial Analyses

To assess how watershed characteristics influence patterns in hydrochemistry across our YKD study sites, we determined watershed area, terrain elevation and slope, and vegetation productivity. We used the ArcticDEM digital surface model (DSM) (Porter et al., 2018) to delineate watershed boundaries. First, sinks in the DSM were filled following (Wang & Liu, 2006) and then a flow accumulation raster was created from the filled DSM using software SAGA v2.3.1. Next, water sampling locations were snapped to the highest flow point within 50 m using the software QGIS v2.18 tool *snap-points-to-grid*. Snapped points were adjusted manually, as needed, to ensure the correct pour-points for each sampled waterbody. Finally, watershed boundaries were generated using the filled DSM for each sample pour-point using the SAGA algorithm *Upslope Area.* Information on vegetation productivity and water extent was derived from Sentinel-2A multispectral surface reflectance imagery (10-m resolution) obtained from Copernicus Sentinel data (European Space Agency, https://sentinel.esa.int/, last access: 01 March 2020). The modified Normalized Difference Vegetation Index (NDVI) and Normalized Difference Water Index (NDWI), metrics of vegetation productivity and canopy or soil moisture, were derived from a composite of cloud-free Sentinel-2A imagery collected from 2017 to 2019 within 2 weeks of most sample collection dates (early July). Elevation was obtained from the ArcticDEM, from which we calculated watershed slope using the algorithm *ee.Terrain.slope* in Google Earth Engine (GEE) (Gorelick et al., 2017). Using the elevation, slope, and Sentinel-2A, we created an image classification using Weka k-means (*ee.Clustere.wekaKMeans* in GEE) to map surface water in the region. We then calculated watershed averages of NDVI, NDWI, and slope using *ee.Image.reduceRegion* with *ee.Reducer.mean* in GEE, first using the *updateMask* function to mask surface waters. Geospatial data for wildfire burn areas were obtained from the Alaska Interagency Coordination Center (https://fire.ak.blm.gov/). Watersheds with ≤10% burned area were designated as "unburned" and those with >10% were "burned".

2.5. Statistical Analyses

We used the non-parametric permutational analysis of variance (permANOVA) to test for (a) effects of recent wildfire on surface water quality and chemistry within each of the five aquatic environments (e.g., burned vs. unburned plateau ponds) and (b) differences in hydrochemistry among landscapes sharing the same recent burn histories (e.g., burned plateau ponds vs. burned fen pond). When results from (a) were significant or striking,

larger sample sizes for lakes and fen ponds during 2016–2019 allowed us to assess post-fire multi-year variation in aquatic chemistry (e.g., burned vs. unburned, by year) using permANOVA (years with three or fewer observations values were excluded). permANOVA randomly permutes the variables within a data set (1,000 times in this study) to generate an empirical pseudo *F*-value distribution, relaxing the assumption that errors are normally distributed (Anderson, 2001). We implemented permANOVA using the *aovp* function in the R software package *lmPerm* (Wheeler & Torchiano, 2016). For each hydrochemical parameter, we included aquatic environment, wildfire history, and their interaction as covariates. A *post-hoc* Tukey's honest significant difference test was performed on significant results to determine differences among aquatic environments. As needed, the dependent (hydrochemistry) variable was first log-transformed to improve homogeneity in variances among treatment groups (i,e., aquatic environment and burn history). We focus on comparisons within individual aquatic environments having different burn histories (e.g., plateau burned vs. plateau unburned), and on different aquatic environments sharing a common recent burn history (e.g., lakes and plateaus in unburned watersheds). We used the same approach to investigate variation in pore water quality and chemistry among burned and unburned plateau ponds and fens.

To characterize relationships in hydrochemical parameters among landscape types, we used the multivariate principal components analysis (PCA). First, to assess geochemical differences across landscapes, we conducted a PCA on both burned and unburned surface water samples from fens (both ponds and channels), lakes, plateaus, and streams. We included hydrochemical variables for water quality (temperature, conductivity, pH, D.O. (%)), concentrations of nutrients (DOC, NH_4^+, NO_3^-, PO_4^{3-}) and gasses (CO_2, CH_4), and carbon quality ($SUVA_{254}$). We removed any missing values from the data set, standardized the variables (mean = 0, SD = 1), and then assessed the correlation matrix using euclidean distance. We used *envfit* (in the 'vegan' package) (Oksanen et al., 2018) to test for the significance of the geochemical vectors using 999 permutations, then also tested supplementary environmental variables including NDVI, slope, and watershed area, as well as year, month, burn status, and landscape type.

Second, to evaluate the effect of wildfire on multiple geochemical variables within a landscape type, we completed a PCA on the lake data set and fen data set individually. For the lake data set, we used surface water samples and followed the same approach as described above. The fen data set included both ponds and channels, and we used the same approach as above with the following changes: we included both pore water and surface water samples, removed the environmental variables of NDVI, slope, and area (due to missing data), then added water sample type (surface or pore water) as an environmental factor.

In a summary table, we present statistics (mean ± standard error) for each of the five aquatic environments and separated by burn history (i.e., unburned, burned). In the text, we specify where means were calculated for unburned and burned sites together. Differences are reported as significant for $p \leq 0.05$ and all statistics were performed using R software v.3.4.4 (R Core Team, 2018). Field sampling was intentionally designed to investigate spatial patterns in hydrochemistry among aquatic environments, rather than to test for potential effects from seasonal thaw.

3. Results

3.1. Landscape Characteristics

The five aquatic environments were located along a broad landscape gradient, whereby plateau ponds and fen ponds were located within smaller watersheds and at higher elevations, lakes were intermediate in landscape position and watershed area, and fen channels and streams were lower in the landscape and drained larger areas (Figure S1 in Supporting Information S1). Watershed slope (m m^{-1}) was lowest for plateau ponds (1.4) and similar for the other environments (1.9–2.1). Watershed NDVI was lowest for plateau ponds (0.31), highest for fen ponds (0.39), and similar among the environments (0.36).

3.2. Surface Water Chemistry Across Aquatic Landscape Environments

3.2.1. Conductivity, pH, and Dissolved Oxygen

Mean surface water conductivity ranged from 29.8 to 34.9 μS cm^{-1}, and results from the permANOVA showed that conductivity did not vary significantly among the aquatic environments (Table 1). Conductivity was,

Table 1
Mean ± Standard Error for Surface Water Chemical Parameters in the Five Aquatic Environments

Parameter	Burn history	Plateau pond	Fen pond	Lake	Fen channel	Stream	Aquatic env. *p*
Temperature	Unburned	12.1 ± 0.9	11.5 ± 0.8	16.5 ± 0.5	10.7 ± 1.1	9.6 ± 2.9	<0.001
(˚C)	Burned	11.0 ± 1.0	12.2 ± 0.6	15.5 ± 0.4	12.8 ± 0.8	11.7 ± 1.1	
Conductivity	Unburned	29.4 ± 3.2	31.5 ± 5.0	29.1 ± 1.2	23.4 ± 3.1	21.6 ± 7.3	ns
(μS cm^{-1})	Burned	30.1 ± 3.3	36.2 ± 3.6	39.0 ± 3.2	40.0 ± 4.7	35.5 ± 4.1	
pH	Unburned	5.22 ± 0.17	**4.88 ± 0.11**	6.06 ± 0.06	5.88 ± 0.2	5.6 ± 0.3	<0.001
(pH units)	Burned	5.40 ± 0.09	**5.38 ± 0.06**	6.24 ± 0.06	6.06 ± 0.10	6.24 ± 0.08	
D.O.	Unburned	44.2 ± 6.2	48.0 ± 7.2	**79.2 ± 3.0**	62.8 ± 5.1	57.8 ± 10.1	<0.001
(% saturation)	Burned	53.3 ± 6.9	32.9 ± 4.1	**92.4 ± 1.8**	61.9 ± 6.3	73.8 ± 3.8	
DOC	Unburned	1,576 ± 249	**1,915 ± 207**	1,091 ± 46	1,201 ± 132	1,412 ± 347	<0.001
(μM)	Burned	1,292 ± 205	**1,275 ± 78**	1,096 ± 39	1,407 ± 120	1,244 ± 101	
NH_4^+	Unburned	1.14 ± 0.37	**0.88 ± 0.24**	**2.76 ± 0.28**	2.62 ± 1.12	2.51 ± 2.30	<0.01
(μM)	Burned	2.83 ± 1.72	**1.90 ± 0.26**	**3.11 ± 1.22**	7.73 ± 4.49	4.05 ± 1.09	
NO_3^-	Unburned	1.51 ± 0.23	1.03 ± 0.13	1.76 ± 0.28	1.23 ± 0.19	**0.55 ± 0.31**	<0.001
(μM)	Burned	2.46 ± 0.95	0.74 ± 0.08	2.12 ± 0.66	3.47 ± 0.87	**7.32 ± 2.28**	
PO_4^{3-}	Unburned	0.19 ± 0.02	*0.22 ± 0.03*	0.16 ± 0.01	0.18 ± 0.03	0.17 ± 0.09	<0.001
(μM)	Burned	0.23 ± 0.02	*0.15 ± 0.01*	0.17 ± 0.01	0.24 ± 0.02	0.28 ± 0.04	
CO_2	Unburned	381 ± 86	**418 ± 111**	*64 ± 4*	272 ± 44	473.43	<0.001
(μM)	Burned	371 ± 151	**174 ± 28**	*47 ± 8*	474 ± 109	172 ± 20	
CH_4	Unburned	32.5 ± 14.8	9.3 ± 2.9	2.7 ± 0.3	2.8 ± 0.8	0.5 ± 0.5	<0.01
(μM)	Burned	9.7 ± 5.3	7.2 ± 1.5	2.8 ± 0.7	17.0 ± 5.4	5.4 ± 1.4	
$SUVA_{254}$	Unburned	4.65 ± 0.2	4.43 ± 0.3	5.15 ± 0.25	5.15 ± 1.27	3.24	ns
(L mgC^{-1} m^{-1})	Burned	4.38 ± 0.4	4.28 ± 0.2	4.58 ± 0.25	4.48 ± 0.28	6.04 ± 1.83	
δ^{13}C-DIC	Unburned	−14.7 ± 1.0	−16.7 ± 1.3	−11.1 ± 0.5	−16.4 ± 0.7	−21.5	<0.001
(‰VPDB)	Burned	−16.7 ± 1.5	−16.5 ± 0.4	−9.1 ± 0.5	−16.2 ± 1.2	−12.1 ± 0.7	
δ^{13}C-CH_4	Unburned	−50.9 ± 2.6	−45.0 ± 2.1	−42.8 ± 0.7	−48.8 ± 3.5	−38.8	0.01
(‰VPDB)	Burned	−46.0 ± 2.3	−45.3 ± 1.3	−45.8 ± 0.8	−51.2 ± 1.0	−49.2 ± 1.8	
d-excess	Unburned	8.3 ± 1.7	3.5 ± 1.3	−4.0 ± 0.7	2.1 ± 2.1	5.8 ± 1.6	<0.001
(‰ VSMOW)	Burned	4.6 ± 2.4	3.2 ± 0.6	−6.0 ± 0.6	2.5 ± 1.0	2.5 ± 1.5	

Note. D.O., dissolved oxygen; DOC, dissolved organic carbon; $SUVA_{254}$, specific UV absorbance at 254 nm. Permutational analysis of variance (permANOVA) was used to test for wildfire effects on hydrochemistry in each of the five aquatic environments (e.g., unburned vs. burned plateau ponds) (Section 2.5). Results are reported as **significant** ($p \leq 0.05$), *marginally significant* ($0.05 < p \leq 0.1$), or non-significant ($p > 0.1$). permANOVA was also used to test for differences in hydrochemistry among aquatic environments sharing the same recent burn histories (e.g., lakes and plateau ponds in unburned watersheds). For significant results (column "Aquatic env. *p*"), pairwise comparisons between aquatic environments were determined from a *post-hoc* Tukey honest significant difference and are illustrated graphically for select parameters in Figure 2. ns = not significant.

however, generally (i.e., not always significantly) higher in aquatic environments within burned watersheds. Broadly, aquatic environments with lower pH and D.O. generally had smaller watersheds and were positioned higher in the landscape (Table 1, Figure S1 in Supporting Information S1). Considering burned and unburned watersheds together, pH was, on average, higher in lakes (6.16), streams (6.12), and fen channels (6.0) than in plateau ponds (5.31) and fen ponds (5.23). pH was significantly higher in burned fen ponds, on average, higher in aquatic environments within burned watersheds (Figure 2a). D.O. (%) was highest in lakes (86.9), intermediate for streams (70.8) and fen channels (62.2), and lower in plateau ponds (49.0) and fen ponds (37.4). Similar to pH, D.O. was generally higher within burned watersheds, except for fen ponds. Wildfire effects on D.O. were

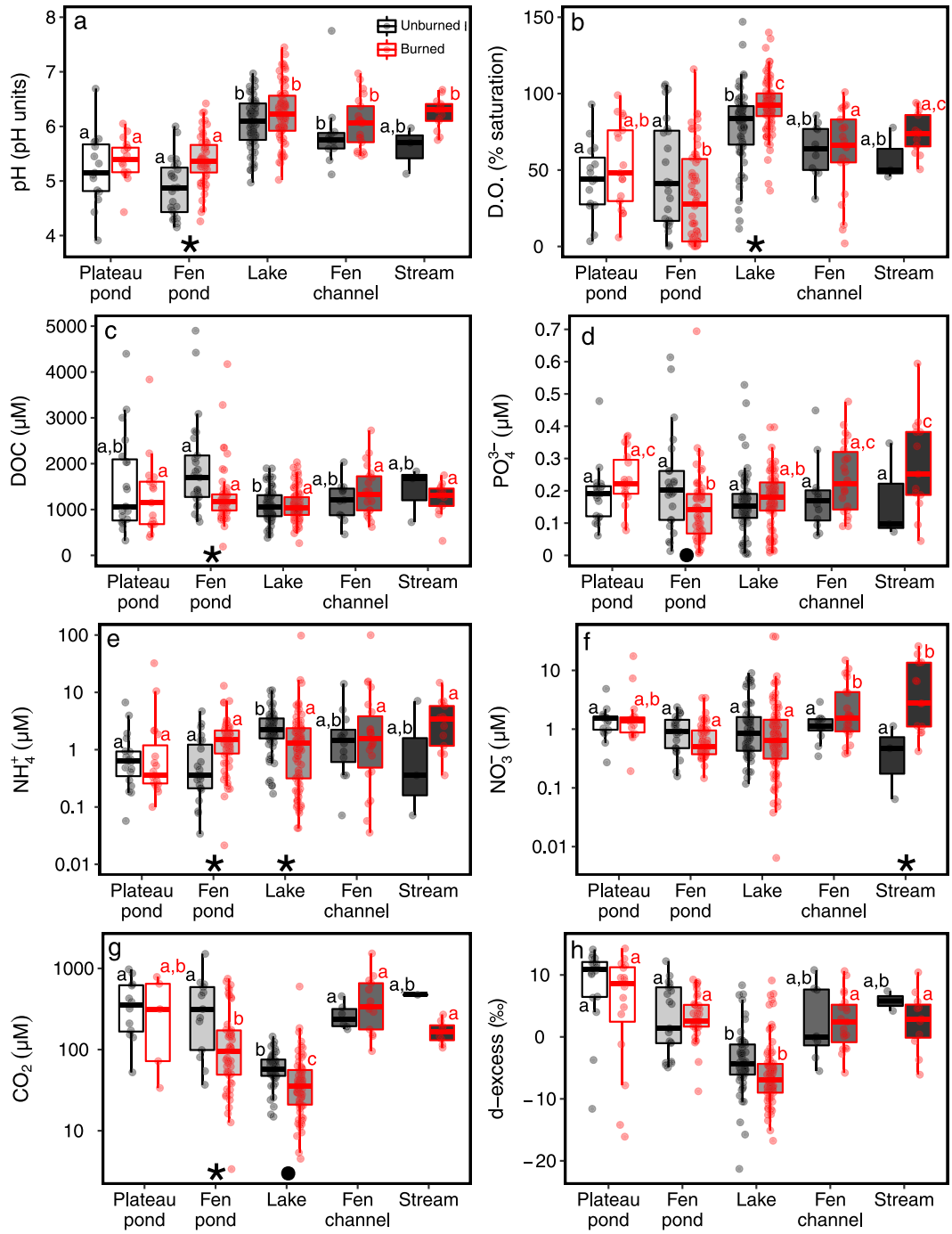

Figure 2. Surface water quality (a–b) and concentrations of dissolved organic carbon (c), nutrients (d–f), and CO_2 (g), and d-excess (h) in the five aquatic environments. Each site type is shaded differently, to help visualize and differentiate. Considering aquatic environments within unburned and burned watersheds separately, boxes with different letters reflect significantly different mean values (e.g., pH in fen ponds and lakes within burned watersheds), as determined by permANOVA (Section 2.5). Note: Letters above boxes are color-coded by burn history. Along the x-axis, * and • reflect statistically significant ($p < 0.05$) and marginal ($0.5 < p \leq 0.1$) differences between unburned and burned sites within the corresponding aquatic environment (e.g., D.O.% within burned vs. unburned lakes). Horizontal line within each box represents the median. Horizontal lines below and above the median represent the first and third quantiles, respectively. Lower and upper whiskers extend from the first or third quantile to the smallest or greatest value, respectively, to no more than 1.5 times the inter-quantile range. All values, including outliers beyond the whiskers, are shown as individual points.

significant only for lakes (Figure 2b). These results also show wildfire in the YKD was associated with more oxygenated and buffered aquatic environments (elevated pH and conductivity).

3.2.2. Carbon and Inorganic Nutrient Concentrations

Mean concentrations of DOC, NH_4^+, NO_3^-, and PO_4^{3-} and the effects of wildfire varied significantly among aquatic environments (Table 1). Among landscape types (not accounting for burn history), mean DOC (μM) was highest in fen ponds (1466) and plateau ponds (1442), intermediate in fen channels (1336) and streams (1276), and lowest in lakes (1094). Wildfire was associated with lower DOC in plateau ponds, fen ponds, and streams; no strong effect in lakes; and increased DOC in fen channels (Table 1). Only fen ponds showed a significant difference in DOC associated with burn history. Among aquatic environments, mean NH_4^+ ranged from 1.6 to 5.9 μM and was highest in fen channels and lowest in fen ponds. For all aquatic environments, NH_4^+ was higher in burned watersheds (Table 1, Figure 2d), but only significantly higher in burned lakes and fen ponds. Mean NO_3^- (μM) was highest in streams (6.1), intermediate in plateaus, fen channels, and lakes (2.0–2.7), and lowest in fen ponds (0.8) (Table 1, Figure 2e). NO_3^- was higher in burned environments, except for fen ponds. Mean PO_4^{3-} ranged from 0.17 to 0.26 μM and was higher in burned environments except for fen ponds (Figure 2f). Together, these results show that wildfire generally decreased concentrations of DOC and increased NH_4^+, NO_3^-, and PO_4^{3-}.

3.2.3. CO_2 and CH_4 Concentrations and Fluxes

CO_2 concentrations and fluxes were significantly different among aquatic environments (Table 1). Regardless of burn status, CO_2 concentrations (μM) were highest in fen channels (410) and plateau ponds (378), intermediate in fen ponds (223) and streams (205), and lowest in lakes (53). CO_2 concentrations and instantaneous CO_2 fluxes followed similar patterns among environments. CO_2 fluxes (μmol m^{-2} s^{-1}) were highest in fen channels (1.78), intermediate in fen ponds (0.97) and plateau ponds (0.95), and lowest in streams (0.42) and lakes (0.15). Wildfire was generally associated with lower CO_2 concentrations in all environments with the exception of fen channels (Table 1). Differences associated with burn status were only significant for fen ponds (Figure 2g). Only fen channels had higher CO_2 concentrations in burned sites than in unburned sites (474 vs. 272 μM). Although CO_2 fluxes were generally lower in burned watersheds, the difference was not significant for any aquatic environments (Table S2 in Supporting Information S1). These results show a strong coupling between CO_2 concentrations and fluxes across watershed types, higher CO_2 concentrations in upland aquatic environments with smaller watershed areas, and a general reduction in CO_2 associated with wildfire.

CH_4 concentrations (μM) were also significantly different among aquatic environments. CH_4 was highest in plateau ponds (23.0), intermediate in fen channels (12.3), and lower in fen ponds, streams, and lakes (2.7–7.7). Compared to CO_2, CH_4 fluxes did not appear as strongly correlated with CH_4 concentrations and CH_4 fluxes overall showed greater variability (higher variability relative to the mean) (Table 1). CH_4 fluxes (nmol m^{-2} s^{-1}) were highest from fen channels (80.8), intermediate from fen ponds (49.0), lakes (40.0) and plateau ponds (37.9), and lowest from streams (15.0). There were no clear trends in CH_4 concentrations or fluxes between unburned and burned sites (Table S2 in Supporting Information S1). Broadly, these results show that CH_4 concentrations and fluxes were not as strongly coupled or as clearly affected by wildfire as CO_2, yet CH_4 concentrations followed a similar pattern among landscape types and were generally higher in upland aquatic environments within smaller watersheds, and highest in pore waters.

3.2.4. Indices of the Composition of DOC, DIC, CH_4, and H_2O

$SUVA_{254}$ was generally higher in unburned watersheds, but did not vary significantly across aquatic environment type or wildfire history (Table 1). The stable isotopic compositions of DIC, CH_4, and H_2O showed greater variation. δ^{13}C-DIC values (‰) were generally lower in plateaus, fen ponds, and fen channels (−15.2 to −16.6) than in streams (−13.3), and lakes (−9.8) (Figure 3). δ^{13}C-DIC values were generally higher in lakes and streams within burned watersheds, except for plateau ponds. Mean δ^{13}C-CH_4 values (‰) among the aquatic environments ranged from −44.9 in lakes to −50.4 in fen channels. Compared to δ^{13}C-DIC, δ^{13}C-CH_4 varied more modestly among aquatic environments and did not reflect consistent effects from wildfire (Table 1, Figure 4). The stable isotopic composition of H_2O in surface waters deviated from the GMWL to a varying degree for each aquatic environment (Figure S2 in Supporting Information S1). d-excess (‰) was highest

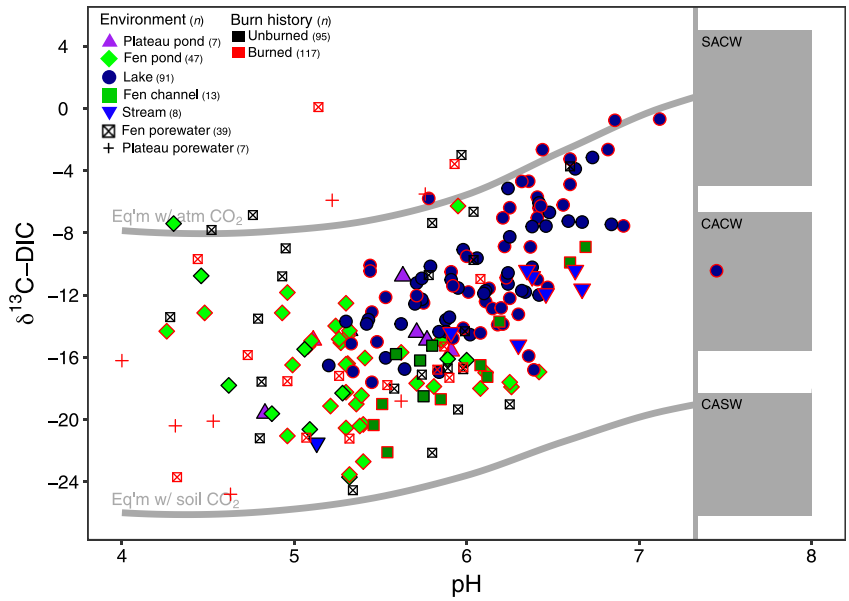

Figure 3. pH and the composition of stable dissolved inorganic carbon isotopes (δ^{13}C-DIC) in aquatic environments within the Yukon Kuskokwim Delta (five surface water, two pore water). Reference lines depict theoretical end-member values for equilibrium reactions with atmospheric and biotic CO_2, which—up to pH ~ 7.3 for these samples—have a greater effect on δ^{13}C-DIC values compared with kinetic isotope fractionation effects from mineral weathering reactions. Proximity to gray areas (pH > 7.3) reflects greater contributions to DIC from H_2SO_4 carbonate weathering (SACW), H_2CO_3 carbonate weathering (CACW), or H_2CO_3 silicate weathering (CASW) (Section 2.3).

for plateau ponds (6.4), intermediate for fen ponds (3.3), streams (3.0), and fen channels (2.4), and lowest for lakes (−5.2), and lower in burned environments except fen channels (Table 1, Figure 2h). In summary, δ^{13}C-DIC results broadly span a gradient of stronger soil-water linkages in fen surface waters and pore waters and stronger water-atmosphere exchange in lakes (irrespective of burn history), while δ^{13}C-CH_4 results suggest

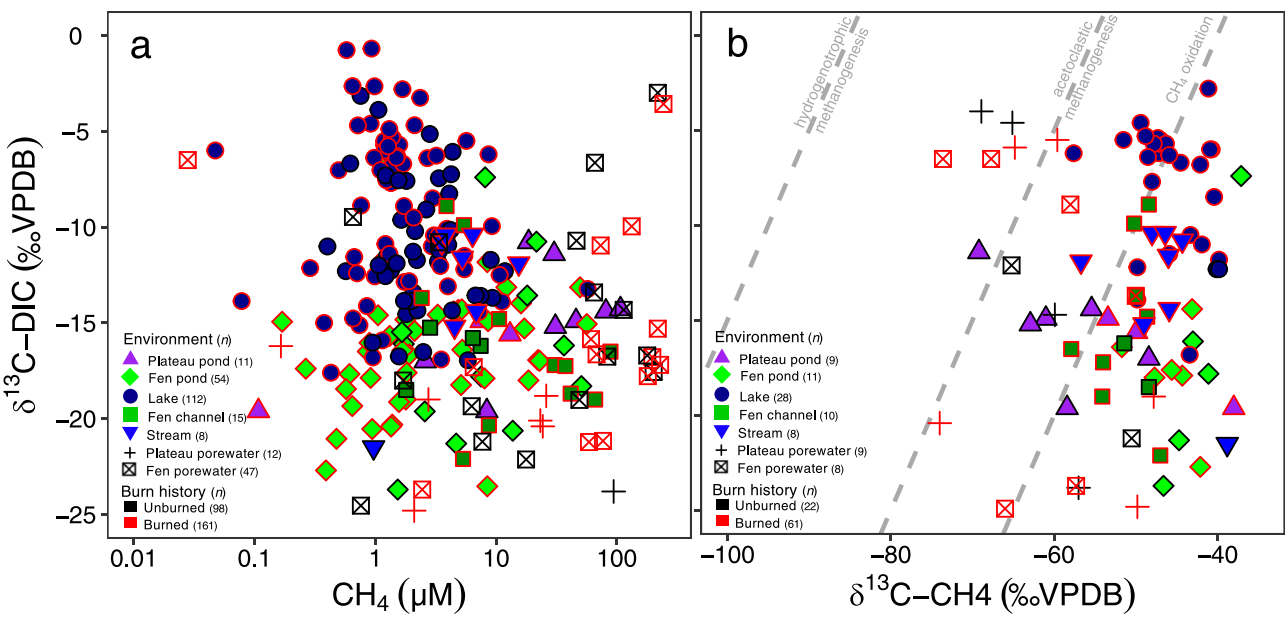

Figure 4. Stable isotopic composition of dissolved inorganic carbon (δ^{13}C-DIC) as a function of (a) CH_4 concentration and (b) the stable isotopic composition of CH_4 (δ^{13}C-CH_4) in surface and pore waters of the Yukon-Kuskokwim Delta. Burn history depicts sites associated with wildfire. Equilibrium fractionation end-members (dotted lines) for methanogenic pathways and methanotrophy after Campeau et al. (2018).

Table 2
Mean ± Standard Error for Pore Water Chemical Parameters in Plateau Ponds and Fens

Parameter	Burn history	Plateau ponds	Fen	*p*
Temperature	Unburned	10.6 ± 1.5	15.4 ± 1.1	<0.01
(˚C)	Burned	9.1 ± 1.2	14.0 ± 1.2	
Conductivity	Unburned	54.5 ± 18.4	121.7 ± 16.1	0.06
(μS cm^{-1})	Burned	83.1 ± 24.2	190.6 ± 56.8	
pH	Unburned	–	5.43 ± 0.14	0.04
(pH units)	Burned	4.87 ± 0.26	5.33 ± 0.14	
D.O.	Unburned	37.3 ± 14.3	24.0 ± 3.7	ns
(% saturation)	Burned	12.1 ± 6.9	29.5 ± 4.4	
DOC	Unburned	1,413 ± 245	2,690 ± 256	0.04
(μM)	Burned	2,539 ± 677	3,661 ± 543	
NH_4^+	Unburned	0.31 ± 0.1	153.8 ± 48.2	<0.001
(μM)	Burned	1.52 ± 0.6	134.8 ± 47.1	
NO_3^-	Unburned	6.9 ± 3.2	1.3 ± 0.4	0.05
(μM)	Burned	68.9 ± 66.2	50.7 ± 39.8	
PO_4^{3-}	Unburned	0.22 ± 0.1	0.82 ± 0.2	<0.01
(μM)	Burned	0.26 ± 0.1	4.06 ± 2.4	
CO_2	Unburned	2,546 ± 424	2,135 ± 231	ns
(μM)	Burned	2,187 ± 899	2,999 ± 381	
CH_4	Unburned	356 ± 93	188 ± 37	ns
(μM)	Burned	151 ± 91	230 ± 44	
$SUVA_{254}$	Unburned	3.93 ± 0.74	3.96 ± 0.48	ns
(L mgC^{-1} m^{-1})	Burned	4.00 ± 0.56	3.87 ± 0.33	
δ^{13}C-DIC	Unburned	−11.8 ± 4.7	−13.1 ± 1.1	ns
(‰VPDB)	Burned	−16.3 ± 2.5	−14.1 ± 1.4	
$\delta^{13}C$-CH_4	Unburned	−64.3 ± 2.6	−57.9 ± 7.4	ns
(‰VPDB)	Burned	−59.2 ± 4.8	−62.1 ± 3.5	
d-excess	Unburned	4.5 ± 2.6	8.4 ± 1.0	ns
(‰ VSMOW)	Burned	8.8 ± 1.8	10.0 ± 1.0	

Note. D.O., dissolved oxygen; DOC, dissolved organic carbon; $SUVA_{254}$, specific UV absorbance at 254 nm. Permutational analysis of variance (permANOVA) was used to test for wildfire effects on hydrochemistry in each landscape category (e.g., unburned vs. burned plateau ponds) (Section 2.5). Results are reported as **significant** ($p \leq 0.05$), *marginally significant* ($0.05 < p \leq 0.1$), or non-significant ($p > 0.1$). permANOVA was also used to test for differences in hydrochemistry between plateau ponds and fens sharing the same recent burn histories (e.g., plateau ponds and fends in unburned watersheds). For significant results (column "*p*"), pairwise comparisons between plateau ponds and fen were determined from a *post-hoc* Tukey honest significant difference. ns = not significant.

that methane concentrations at most sites were controlled by oxidation (see Section 4.1).

3.3. Pore Water Chemistry in Plateau Ponds and Fens

Compared with plateau ponds and fen surface water, pore water generally had higher conductivity, DOC, TDN, PO_4^{3-}, CO_2, and CH_4, and lower pH, D.O., and $SUVA_{254}$ (Tables 1 and 2). Wildfire was generally associated with higher concentrations of pore water DOC, inorganic nutrients (NH_4^+, NO_3^-, PO_4^{3-}), CO_2, and more positive d-excess values in plateau ponds and fens (Table 2). Similar to plateau ponds and fen surface waters, relatively lower δ^{13}C-DIC and $\delta^{13}C$-CH_4 values indicated that carbon cycling in pore waters was more strongly associated with biotic processes in soils, with some influence from abiotic processes (e.g., CO_2 exchange with the atmosphere) (Figures 3 and 4).

3.4. Wildfire, Terrestrial-Aquatic Connectivity, and Carbon and Nutrient Cycling

The PCA (Figure 5) demonstrated that variation in surface water chemistry was more strongly associated with landscape type than with wildfire effects (Table 1). The first principal component (PC1) explained 28% of the variance, and separated surface waters in lakes and streams from fens and plateaus. Across PC1, lakes showed a strong positive correlation with D.O., temperature, and $SUVA_{254}$, a moderate positive correlation with pH, and a negative correlation with concentrations of DOC, CO_2, and CH_4. In contrast to lakes, fens and some plateau ponds were positively correlated with DOC, CO_2, CH_4, and conductivity. These trends in PC1 indicate that plateau ponds and fens (ponds and channels together) were more strongly correlated with organic carbon processing. The second principal component (PC2) accounted for 15% of the variance, separating streams from the other landscape types. Across PC2, streams showed a positive correlation with concentrations of NH_4^+, NO_3^-, and PO_4^{3-}, indicating a relatively strong association with inorganic nutrient cycling. The *envfit* test found that watershed area, year and landscape type were statistically significant ($p < 0.05$). We further explore multi-year post-fire variation in Section 3.5.

The PCAs of the individual lake and fen datasets, which had more samples, elucidate wildfire effects on hydrochemistry within these two landscape types. In the lake PCA, the burned and unburned samples showed moderate separation across both principal component axes (Figure 6a). Across PC1, unburned sites were generally correlated with higher concentrations of DOC, CO_2, and CH_4, while burned sites were correlated with higher D.O. (%). Across PC2, some burned samples showed strong positive correlations with conductivity, pH, NO_3^-, and PO_4^{3-}. The *envfit* test found that NDVI, sample year and burn status were statistically significant ($p < 0.05$). In the fen PCA, PC scores showed general overlap of burned and unburned samples from surface waters (Figure 6b). However, there was modest separation between surface water and pore water. Across PC1, pore water samples were more strongly correlated with DOC, CO_2, conductivity, CH_4, and to a lesser extent, PO_4^{3-} and temperature. Conversely, surface water samples were correlated with $SUVA_{254}$ and D.O., and to a lesser extent, NO_3^-. There was strong overlap of burned, unburned, pore water and surface water samples across PC2. The *envfit* test found that both the year of sample collection and the water sample type (pore water or surface

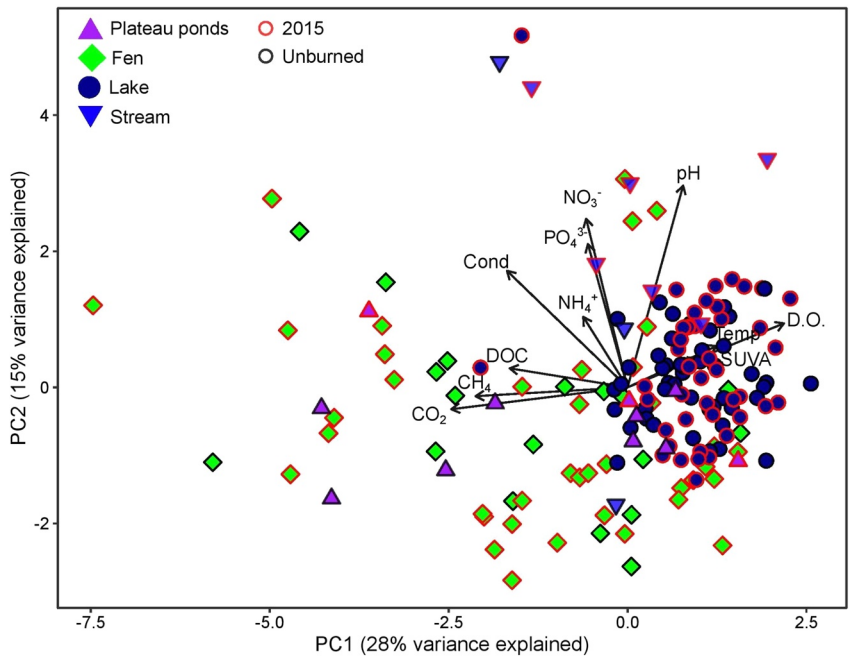

Figure 5. Principal component analysis of surface water geochemical variables for all landscape types. The shapes distinguish between plateau ponds, lakes, fens, and streams, while the border color represents control or burned in 2015. All vectors were multiplied by 5 to improve visibility.

water) were found to be statistically significant ($p < 0.05$). The lake and fen measurements show that variation in surface water chemistry appeared more strongly associated with environmental conditions (Table 1) and provide evidence that landscape type has a greater influence than wildfire on most surface water hydrochemical constituents.

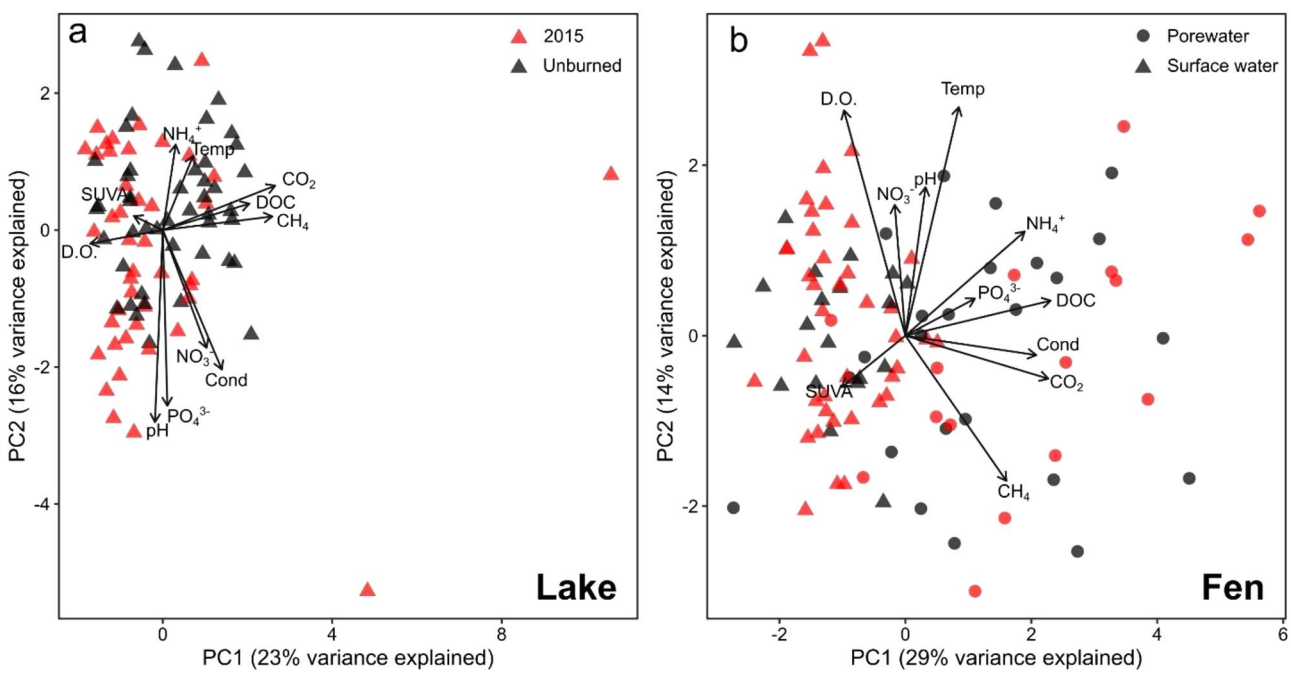

Figure 6. Principal component analysis of geochemical variables for (a) surface water samples from lakes and (b) both surface water and pore water samples from fens. Colors denote burn status (a and b) while shape distinguishes between pore water and surface water samples (b only). All vectors were multiplied by 5 to improve visibility.

3.5. Multi-Year Post-Fire Variation in Lake and Fen Pond Water Chemistry

Strong differences in thaw-season hydrochemistry between unburned and burned lakes (conductivity, D.O., NH_4^+, CO_2) and fen ponds (pH, DOC, NH_4^+, CO_2) (Section 3.2) were, in part, associated with post-fire multi-year variation in these constituents. Lakes within burned watersheds had elevated conductivity compared to unburned sites in the 2 years immediately following wildfire, which tapered in later years (Figure 7a). Dissolved oxygen varied among years and was higher in burned watersheds in 2018 (Figure 7b). Post-fire NH_4^+ varied and was not significantly different between burned and unburned sites for any individual year, despite being significantly higher in burned sites when considering all years together (Table 1) (Figure 7c). Concentrations of CO_2 were consistently lower in lakes within burned watersheds for 3 years post-fire, but differences between burned and unburned sites in each year were not significant due to lower *n* when considering years separately rather than together (Section 3.2) (Figure 7d).

In fen ponds, wildfire was associated with significantly higher pH during the following two summers (Figure 7e). DOC in fen ponds was consistently, but not significantly, lower within burned watersheds for 3 years following wildfire (Figure 7f), whereas NH_4^+ varied (Figure 7g). Fen pond CO_2 was generally lower within burned watersheds in the years following fire and, in 2018, was significantly lower in burned watersheds than in unburned (Figure 7h).

4. Discussion

4.1. Patterns in Hydrochemistry Among Varied Aquatic Environments in a Northern Delta

In the YKD, patterns in surface water hydrochemistry across aquatic environments reveal how landscape factors underlie variation in biogeochemical cycling, irrespective of burn history. Smaller watersheds at higher elevations harbored plateau ponds and fen ponds, where relatively acidic, low-oxygen, and high-DOC and CO_2 surface and pore waters reflect intensified organic carbon cycling driven by strong terrestrial-aquatic linkages and potentially higher soil carbon stocks. In such environments, anoxic, organic-rich conditions may promote CH_4 production in the absence of terminal electron acceptors that are known to inhibit methanogenesis (e.g., NO_3^-, SO_4^{2-}) (Stanley et al., 2016), which may explain why δ^{13}C-CH_4 indicated relatively stronger effects from methanogenesis in pore-waters (Figure 4). Yet, this effect appeared modest and without relation to wildfire history, and our measurements of δ^{13}C-CH_4 indicated stronger effects on CH_4 from oxidation than methanogenesis, for all sites and in both pore and surface waters. While obtained from local observations, these findings suggest that microbial oxidation of CH_4 is likely prevalent in similar environments across the YKD and thus emphasizes the utility of *in-situ* hydrochemical and isotopic measurements for constraining sources and magnitudes of CO_2 and CH_4 emissions at regional scales (Elder et al., 2020). Compared with the other aquatic environments, water isotopes in plateau ponds and fen ponds more closely resembled precipitation (d-excess, Table 1). This agreed with our field observations that rainfall enlarges plateau ponds and suggests that precipitation promotes land-freshwater linkages and the biotic processes that drive organic carbon cycling and relatively high rates of CO_2 and CH_4 efflux in these upland environments of the YKD. While plateau ponds and fen ponds may currently span only a fractional area of the watershed surface, their contributions to net ecosystem exchange may be important, especially if nutrient cycling in these environments is enhanced due to increased rainfall in southwestern Alaska in the coming decades (Lader et al., 2017).

In contrast to fens and plateau ponds, the hydrochemistry of lakes indicated biogeochemical cycles driven by a different suite of processes. Relatively high D.O. and δ^{13}C-DIC values, which more closely resembled the stable isotopic composition of atmospheric CO_2 (−8‰) than biogenic CO_2 (~−22‰) (Kendall et al., 2014), indicated stronger effects on dissolved gases from mixing between lake waters and the atmosphere than from inputs of soil CO_2 from DOC-rich pore waters. Low d-excess values indicate greater effects from evaporation on lake waters (Jasechko, 2019) and perhaps also longer water residence times compared with the relatively more ephemeral plateau ponds and fen ponds. The intermediate hydrochemistry of fen channels and streams, which connect to fen ponds and lakes, respectively, indicated additional hydrologic inputs to these fluvial components of the aquatic network. For instance, streams were more strongly associated with inorganic nutrients, especially NO_3^-, perhaps associated with nitrogen fixation by riparian alders and its subsequent nitrification and hydrologic export into streams (McCaully et al., 2021).

4.2. Wildfire Effects on Hydrochemistry

Superimposed on the variation in hydrochemistry among aquatic environments (Section 4.1), certain water quality and chemistry parameters within individual aquatic environments showed differences associated with recent

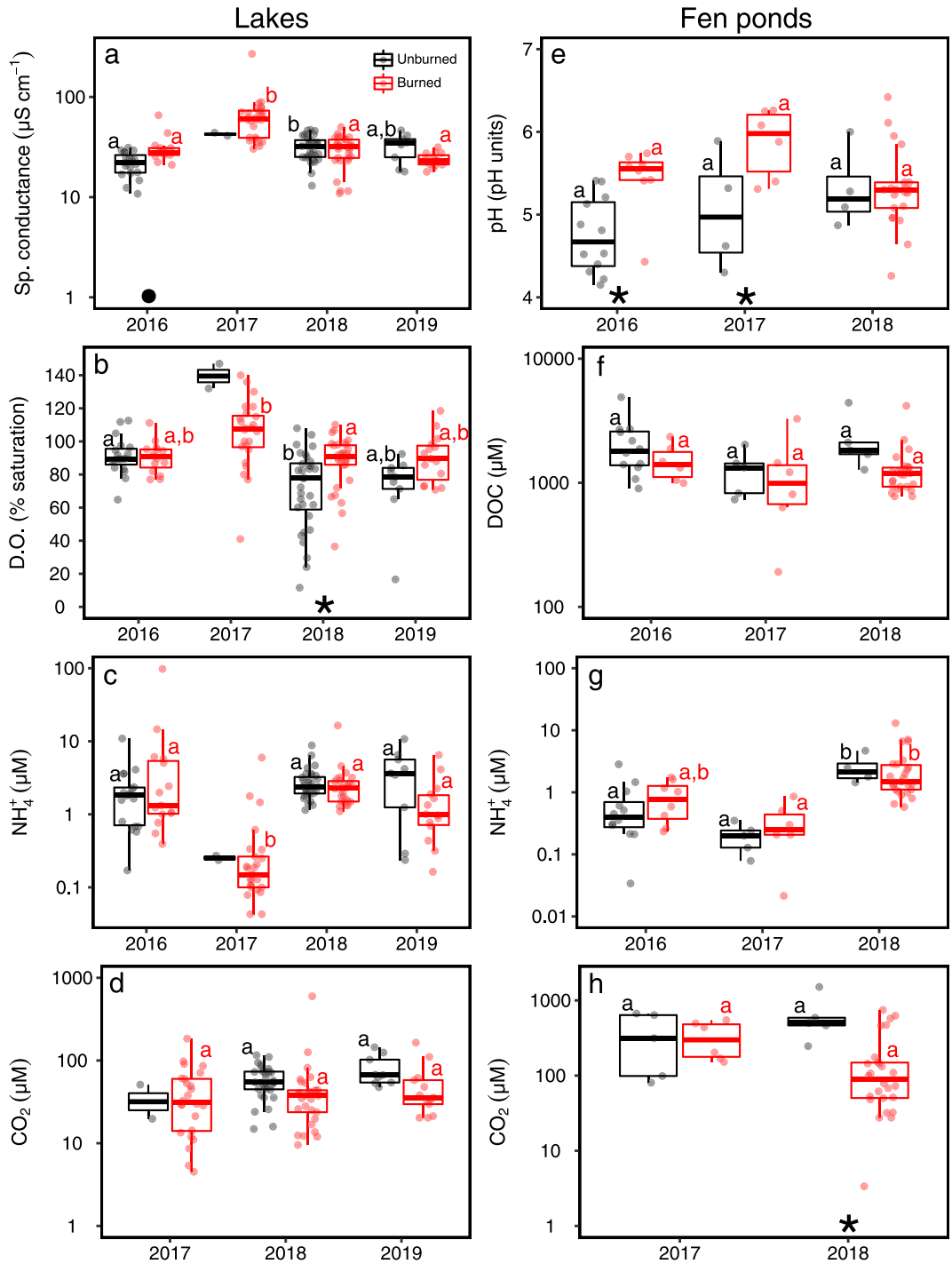

Figure 7. Surface water chemistry in lakes (a–d) and fen ponds (e–h). Considering sampling year within unburned and burned watersheds separately, boxes with different letters reflect significantly different mean values (e.g., specific conductance lakes within burned watersheds during 2017 vs. other years), as determined by permANOVA (Section 2.5). Note: Letters above boxes are color-coded by burn history. Along the x-axis, * and • reflect statistically significant ($p < 0.05$) and marginal ($0.5 < p \leq 0.1$) differences between unburned and burned sites within the corresponding aquatic environment (e.g., pH within burned vs. unburned fen ponds in 2016 and 2017). Horizontal line within each box represents the median. Horizontal lines below and above the median represent the first and third quantiles, respectively. Lower and upper whiskers extend from the first or third quantile to the smallest or greatest value, respectively, to no more than 1.5 times the inter-quantile range. All values, including outliers beyond the whiskers, are shown as individual points.

burn history. Wildfire did not appear to drive variation in hydrochemistry among landscape types, even when considering results for the more intensively-sampled lake and fen environments (Figure 6). Rather, wildfire was associated with general increases in conductivity, pH, D.O., NH_4^+, NO_3^-, PO_4^{3-}, and decreases in DOC and CO_2. These results suggest that wildfire in YKD tundra may have three important ecological functions. First, combustion of organic matter decreases soil organic carbon stocks and soil heterotrophic respiration, thereby reducing DOC and CO_2 inputs to surface waters (Ludwig et al., 2022). Second, wildfire increases the mobilization of cations from soils, evidenced by consistently higher conductivity and pH among all aquatic environments (Table 1). This may be attributed to the release of exchangeable cations following combustion of soil organic matter, where acidity from mobilized anions associated with organics (e.g., SO_4^{2-}) does not counterbalance increased pH (Granath et al., 2021), and/or to thaw-induced deepening of hydrologic flowpaths into solute-rich layers at the freezing front or within permafrost (Lehn et al., 2017; Reyes & Lougheed, 2015). Third, wildfire enhances nitrogen cycling, as indicated by increased NH_4^+ and NO_3^-, perhaps due to biotic processing and hydrologic export of thawed permafrost nitrogen (Abbott et al., 2021). These trends were generally consistent among aquatic environments and the lack of statistical significance in our relatively large data set is taken to reflect variation in the resilience of YKD aquatic environments to the effects of wildfire, as observed in tundra environments elsewhere (Larouche et al., 2015).

Our findings from YKD upland tundra in southwest Alaska help to bolster the narrative of wildfire effects on northern ecosystems, which is growing in both scope and complexity. Similar to this study, physiographic variation was a particularly important driver of variation in lake hydrochemistry among boreal watersheds with contrasting wildfire histories (Lewis et al., 2014; Robinne et al., 2020). Hydrology is an important component of this physiographic variation and is certain to influence patterns in wildfire effects on aquatic biogeochemistry across spatial scales. For instance, lakes in the boreal plains of Alaska are thought to be fed by groundwater, which may circumvent interacting with burned surface soils and thus limit wildfire effects on lake DOC concentrations (Robinne et al., 2020). In contrast, discontinuous permafrost across our study sites in the YKD may favor runoff over groundwater inputs to lakes, except where permafrost is absent (Dabrowski et al., 2020). Pre-fire ecosystem characteristics are also important to predicting the degree to which wildfire may affect aquatic biogeochemical cycles. For instance, in boreal Canada, saturated conditions and relatively lower fuel loads in fens muted the effects of wildfire on aquatic biogeochemistry (Bourgeau-Chavez et al., 2020). In boreal ecosystems with relatively more intense nutrient cycling, post-fire effects on aquatic nutrient concentrations and cycling may be minimal (Lewis et al., 2014). We observed an increase in carbon and nutrient concentrations in pore water samples from fens and plateau ponds, which is similar to the increase in solutes and dissolved organic matter in pore waters following a low-severity fire in a discontinuous peat plateau-wetland complex in the Northwest Territories, Canada (Ackley et al., 2021). Our results for the YKD and observations elsewhere (e.g., Central Siberian Plateau) indicate increased post-fire inorganic nitrogen concentrations (Rodríguez-Cardona et al., 2020). Together, these results highlight that physiographic variation underlies complex spatial and temporal trends in wildfire effects on northern aquatic biogeochemistry.

4.3. Multi-Year Effects of Wildfire on Aquatic Biogeochemistry

In addition to physiographic controls underlying wildfire effects on aquatic biogeochemistry in the YKD, more intensive sampling campaigns in lakes and fen ponds allowed us to evaluate and compare multi-year wildfire effects in two environments characterized by relatively distinct modes of nutrient cycling (Sections 4.1 and 4.2). Our multi-year results for lakes and fen ponds suggest that organic matter combustion by wildfire reduces organic carbon mobilization into the dissolved phase and associated microbial production of CO_2 for at least several years (Figure 7). This is in contrast to other studies in Canadian boreal environments, which found no effect of wildfire on lake DOC (Olefeldt et al., 2013). Among the most striking effects of wildfire on hydrochemistry were increased conductivity in lakes and pH in fen ponds during the summer following wildfire (2016). These patterns may reflect the mobilization of ions from combusted soils (Ludwig et al., 2018), from greater interaction between surface runoff and deeper mineral soils due to active layer thickening, and/or from enhanced groundwater inputs associated with permafrost degradation (Dabrowski et al., 2020). Preliminary results from a study on post-fire primary production in YKD lakes found that PO_4^{3-} was limiting to phytoplankton (Bradley et al., 2019), suggesting that primary production stimulated by increased PO_4^{3-} in wildfire-affected YKD lakes (Table 1) may reduce CO_2. The varied multi-year patterns in NH_4^+ suggest that interannual variability in climate and hydrologic

conditions more strongly influences the response of inorganic nutrients to wildfire, despite our observations that, overall, wildfires in the YKD appear to increase NH_4^+ and NO_3^- in freshwaters.

Overall, multi-year patterns in lake and fen pond hydrochemistry reveal relatively striking post-fire effects on some ecosystem processes, and that aquatic ecosystem response to wildfire disturbance is coupled to effects on connected terrestrial ecosystems. Similar conclusions were made for wildfire-affected boreal and tundra environments elsewhere in North America, where watershed characteristics were key in determining ecosystem response to wildfire (Abbott et al., 2021; Larouche et al., 2015; Robinne et al., 2020). Together, these findings emphasize that wildfire effects on ecosystem nutrient dynamics can propagate across the terrestrial–aquatic continuum. As wildfire activity intensifies at northern high latitudes (Young et al., 2017; Yue et al., 2015) there is strong potential for cascading effects on aquatic ecosystems. Future research in varied physiographic regions across the circumpolar north is needed to refine understanding of potential consequences for northern high latitude biogeochemical cycles.

5. Conclusion

In this study, we analyzed surface and pore water samples from five aquatic environments in tundra of the YKD, Alaska, to assess recent wildfire effects on biogeochemistry. Patterns in hydrochemistry revealed physiographic controls underlying variation among aquatic environments in the YKD: higher-elevation environments in smaller watersheds (plateau ponds, fen ponds) reflected stronger organic carbon cycling and terrestrial-freshwater linkages, whereas lakes were influenced by mixing with the atmosphere, and riparian corridors enhanced inorganic nitrogen export via streams. Wildfire effects varied in strength and among aquatic environments, but broadly influenced aquatic ecosystems by reducing DOC and CO_2 inputs to surface waters, increasing chemical weathering, and enhancing nitrogen cycling. This study is among the first to test for multi-year effects on tundra aquatic biogeochemistry in the year immediately following wildfire, and suggests that wildfire effects on some hydrochemical constituents may persist beyond three to 4 years (DOC, CO_2), while others appear to return to baseline conditions within several years (e.g., conductivity). Climate change is projected to increase the severity and frequency of northern high latitude fires, and the post-fire response of biogeochemical cycles will depend on terrestrial-aquatic connectivity of affected environments and, at broader spatial scales, regional variation in physiographic conditions.

Conflict of Interest

The authors declare no conflicts of interest relevant to this study.

Data Availability Statement

Data used in this study are publicly accessible via the Arctic Data Center (Zolkos et al., 2022). Code is available at https://zenodo.org/badge/latestdoi/235470761.

Acknowledgments
The authors acknowledge and are grateful for the opportunity to conduct research on traditional lands of the Yup'ik, who have stewarded this land for generations. This study was supported by National Science Foundation grants (NSF 1915307, 1624927 to S.M.N., P.M., J.D.S.; 1561437 to S.M.N. and J.D.S) and the Gordon and Betty Moore Foundation (#8414 to S.M.N.). This work would not have been possible without the efforts of the Polaris Project undergraduate students from 2015 to 2019 that aided in sample collection and processing. The authors thank Greg Fiske for sharing expertise on Google Earth Engine.

References

Abbott, B. W., Rocha, A. V., Shogren, A., Zarnetske, J. P., Iannucci, F., Bowden, W. B., et al. (2021). Tundra wildfire triggers sustained lateral nutrient loss in Alaskan Arctic. *Global Change Biology*, *27*(7), 1408–1430. https://doi.org/10.1111/gcb.15507

Ackley, C., Tank, S. E., Haynes, K. M., Rezanezhad, F., McCarter, C., & Quinton, W. L. (2021). Coupled hydrological and geochemical impacts of wildfire in peatland-dominated regions of discontinuous permafrost. *Science of the Total Environment*, *782*, 146841. https://doi.org/10.1016/j.scitotenv.2021.146841

AICC. (2019). Alaska interagency coordination center predictive services - Maps/Imagery/Geospatial. Retrieved from https://fire.ak.blm.gov/predsvcs/maps.php

Anderson, M. J. (2001). Permutation tests for univariate or multivariate analysis of variance and regression. *Canadian Journal of Fisheries and Aquatic Sciences*, *58*(3), 626–639. https://doi.org/10.1139/f01-004

Bourgeau-Chavez, L. L., Grelik, S. L., Billmire, M., Jenkins, L. K., Kasischke, E. S., & Turetsky, M. R. (2020). Assessing boreal peat fire severity and vulnerability of peatlands to early season wildland fire. *Frontiers in Forests and Global Change*, *3*, 20. https://doi.org/10.3389/ffgc.2020.00020

Bradley, E., Natali, S., Schade, J., Mann, P., Rodriguez-Cardona, B., & Ludwig, S. (2019). *The effects of fire on aquatic phytoplankton of the Yukon-Kuskokwim Delta, Alaska*. Presented at the American Geophysical Union Fall Meeting.

Bret-Harte, M. S., Mack, M. C., Shaver, G. R., Huebner, D. C., Johnston, M., Mojica, C. A., et al. (2013). The response of Arctic vegetation and soils following an unusually severe tundra fire. *Philosophical Transactions of the Royal Society B: Biological Sciences*, *368*(1624), 20120490. https://doi.org/10.1098/rstb.2012.0490

Brown, J., Ferrians, O., Heginbottom, J. A., & Melnikov, E. S. (2002). Circum-Arctic map of permafrost and ground-ice conditions, version 2. NSIDC, [Dataset]. https://doi.org/10.7265/SKBG-KF16

Burd, K., Tank, S. E., Dion, N., Quinton, W. L., Spence, C., Tanentzap, A. J., & Olefeldt, D. (2018). Seasonal shifts in export of DOC and nutrients from burned and unburned peatland-rich catchments, Northwest Territories, Canada. *Hydrology and Earth System Sciences*, *22*(8), 4455–4472. https://doi.org/10.5194/hess-22-4455-2018

Campeau, A., Bishop, K., Nilsson, M. B., Klemedtsson, L., Laudon, H., Leith, F. I., et al. (2018). Stable carbon isotopes reveal soil-stream DIC linkages in contrasting headwater catchments. *Journal of Geophysical Research: Biogeosciences*, *123*(1), 149–167. https://doi.org/10.1002/2017JG004083

Connolly, C. T., Khosh, M. S., Burkart, G. A., Douglas, T. A., Holmes, R. M., Jacobson, A. D., et al. (2018). Watershed slope as a predictor of fluvial dissolved organic matter and nitrate concentrations across geographical space and catchment size in the Arctic. *Environmental Research Letters*, *13*(10), 104015. https://doi.org/10.1088/1748-9326/aae35d

Dabrowski, J. S., Charette, M. A., Mann, P. J., Ludwig, S. M., Natali, S. M., Holmes, R. M., et al. (2020). Using radon to quantify groundwater discharge and methane fluxes to a shallow, tundra lake on the Yukon-Kuskokwim Delta, Alaska. *Biogeochemistry*, *148*(1), 69–89. https://doi.org/10.1007/s10533-020-00647-w

Drake, T. W., Holmes, R. M., Zhulidov, A. V., Gurtovaya, T., Raymond, P. A., McClelland, J. W., & Spencer, R. G. M. (2018). Multidecadal climate-induced changes in Arctic tundra lake geochemistry and geomorphology. *Limnology & Oceanography*, *64*(S1). https://doi.org/10.1002/lno.11015

Elder, C. D., Thompson, D. R., Thorpe, A. K., Hanke, P., Walter Anthony, K. M., & Miller, C. E. (2020). Airborne mapping reveals emergent power law of arctic methane emissions. *Geophysical Research Letters*, *47*(3), e2019GL085707. https://doi.org/10.1029/2019GL085707

Frey, K. E., & McClelland, J. W. (2009). Impacts of permafrost degradation on arctic river biogeochemistry. *Hydrological Processes*, *23*(1), 169–182. https://doi.org/10.1002/hyp.7196

Frost, G. V., Loehman, R. A., Saperstein, L. B., Macander, M. J., Nelson, P. R., Paradis, D. P., & Natali, S. M. (2020). Multi-decadal patterns of vegetation succession after tundra fire on the Yukon-Kuskokwim Delta, Alaska. *Environmental Research Letters*, *15*(2), 025003. https://doi.org/10.1088/1748-9326/ab5f49

Gorelick, N., Hancher, M., Dixon, M., Ilyushchenko, S., Thau, D., & Moore, R. (2017). Google Earth Engine: Planetary-scale geospatial analysis for everyone. *Remote Sensing of Environment*, *202*, 18–27. https://doi.org/10.1016/j.rse.2017.06.031

Granath, G., Evans, C. D., Strengbom, J., Fölster, J., Grelle, A., Strömqvist, J., & Köhler, S. J. (2021). The impact of wildfire on biogeochemical fluxes and water quality in boreal catchments. *Biogeosciences*, *18*(10), 3243–3261. https://doi.org/10.5194/bg-18-3243-2021

Helms, J. R., Stubbins, A., Ritchie, J. D., Minor, E. C., Kieber, D. J., & Mopper, K. (2008). Absorption spectral slopes and slope ratios as indicators of molecular weight, source, and photobleaching of chromophoric dissolved organic matter. *Limnology & Oceanography*, *53*(3), 955–969. https://doi.org/10.4319/lo.2008.53.3.0955

Hesslein, R. H., Rudd, J. W. M., Kelly, C., Ramlal, P., & Hallard, K. A. (1991). Carbon dioxide pressure in surface waters of Canadian lakes. In S. C. Wilhelms & J. S. Gulliver (Eds.), *Air-water mass transfer: Selected papers from the second international symposium on gas transfer at water surfaces* (pp. 413–431). American Society of Civil Engineers.

Holloway, J. E., Lewkowicz, A. G., Douglas, T. A., Li, X., Turetsky, M. R., Baltzer, J. L., & Jin, H. (2020). *Impact of wildfire on permafrost landscapes: A review of recent advances and future prospects*. Permafrost and Periglacial Processes. https://doi.org/10.1002/ppp.2048

Hugelius, G., Loisel, J., Chadburn, S., Jackson, R. B., Jones, M., MacDonald, G., et al. (2020). Large stocks of peatland carbon and nitrogen are vulnerable to permafrost thaw. *Proceedings of the National Academy of Sciences*, *117*(34), 20438–20446. https://doi.org/10.1073/pnas.1916387117

Hutchins, R. H. S., Prairie, Y. T., & del Giorgio, P. A. (2019). Large-Scale landscape drivers of CO_2, CH_4, DOC, and DIC in boreal river networks. *Global Biogeochemical Cycles*, *33*(2), 125–142. https://doi.org/10.1029/2018GB006106

Hutchins, R. H. S., Tank, S. E., Olefeldt, D., Quinton, W. L., Spence, C., Dion, N., et al. (2020). Fluvial CO_2 and CH_4 patterns across wildfire-disturbed ecozones of subarctic Canada: Current status and implications for future change. *Global Change Biology*, *26*(4), 2304–2319. https://doi.org/10.1111/gcb.14960

Jasechko, S. (2019). Global isotope hydrogeology——Review. *Reviews of Geophysics*, *57*(3), 835–965. https://doi.org/10.1029/2018RG000627

Kasischke, E. S., Verbyla, D. L., Rupp, T. S., McGuire, A. D., Murphy, K. A., Jandt, R., et al. (2010). Alaska's changing fire regime — Implications for the vulnerability of its boreal forestsThis article is one of a selection of papers from the dynamics of change in Alaska's boreal forests: Resilience and vulnerability in response to climate warming. *Canadian Journal of Forest Research*, *40*(7), 1313–1324. https://doi.org/10.1139/X10-098

Kendall, C., Doctor, D. H., & Young, M. B. (2014). Environmental isotope applications in hydrologic studies. In H. D. Holland & K. K. Turekian (Eds.), *Treatise on geochemistry* (Vol. 7, pp. 273–327). Elsevier. https://doi.org/10.1016/B978-0-08-095975-7.00510-6

Koch, J. C., Kikuchi, C. P., Wickland, K. P., & Schuster, P. (2014). Runoff sources and flow paths in a partially burned, upland boreal catchment underlain by permafrost. *Water Resources Research*, *50*(10), 8141–8158. https://doi.org/10.1002/2014WR015586

Lader, R., Walsh, J. E., Bhatt, U. S., & Bieniek, P. A. (2017). Projections of twenty-first-century climate extremes for Alaska via dynamical downscaling and quantile mapping. *Journal of Applied Meteorology and Climatology*, *56*(9), 2393–2409. https://doi.org/10.1175/JAMC-D-16-0415.1

Larouche, J. R., Abbott, B. W., Bowden, W. B., & Jones, J. B. (2015). The role of watershed characteristics, permafrost thaw, and wildfire on dissolved organic carbon biodegradability and water chemistry in Arctic headwater streams. *Biogeosciences*, *12*(14), 4221–4233. https://doi.org/10.5194/bg-12-4221-2015

Lehn, G. O., Jacobson, A. D., Douglas, T. A., McClelland, J. W., Barker, A. J., & Khosh, M. S. (2017). Constraining seasonal active layer dynamics and chemical weathering reactions occurring in North Slope Alaskan watersheds with major ion and isotope ($\delta^{34}S_{SO4}$, $\delta^{13}C_{DIC}$, $^{87}Sr/^{86}Sr$, $\delta^{44/40}Ca$, and $\delta^{44/42}Ca$) measurements. *Geochimica et Cosmochimica Acta*, *217*, 399–420. https://doi.org/10.1016/j.gca.2017.07.042

Lewis, T. L., Lindberg, M. S., Schmutz, J. A., & Bertram, M. R. (2014). Multi-trophic resilience of boreal lake ecosystems to forest fires. *Ecology*, *95*(5), 1253–1263. https://doi.org/10.1890/13-1170.1

Littlefair, C. A., & Tank, S. E. (2018). Biodegradability of thermokarst carbon in a till-associated, glacial margin landscape: The case of the Peel Plateau, NWT, Canada. *Journal of Geophysical Research: Biogeosciences*, *123*(10), 3293–3307. https://doi.org/10.1029/2018JG004461

Ludwig, S. M., Alexander, H. D., Kielland, K., Mann, P. J., Natali, S. M., & Ruess, R. W. (2018). Fire severity effects on soil carbon and nutrients and microbial processes in a Siberian larch forest. *Global Change Biology*, *24*(12), 5841–5852. https://doi.org/10.1111/gcb.14455

Ludwig, S. M., Natali, S. M., Mann, P. J., Schade, J. D., Holmes, R. M., Powell, M., et al. (2022). Using machine learning to predict inland aquatic CO_2 and CH_4 concentrations and the effects of wildfires in the Yukon-Kuskokwim delta, Alaska. *Global Biogeochemical Cycles*, *36*(4). https://doi.org/10.1029/2021GB007146

McCaully, R. E., Arendt, C. A., Newman, B. D., Salmon, V. G., Heikoop, J. M., Wilson, C. J., et al. (2021). High temporal and spatial nitrate variability on an Alaskan hillslope dominated by alder shrubs. https://doi.org/10.5194/tc-2021-166

NOAA. (2020). Climate data online. Retrieved from https://www.ncdc.noaa.gov

Oksanen, J., Blanchet, F. G., Friendly, M., Kindt, R., Legendre, P., McGlinn, D., et al. (2018). Package 'vegan' (version 2.4-6). Retrieved from http://CRAN.R-project.org/package=vegan

Olefeldt, D., Devito, K. J., & Turetsky, M. R. (2013). Sources and fate of terrestrial dissolved organic carbon in lakes of a Boreal Plains region recently affected by wildfire. *Biogeosciences*, *10*(10), 6247–6265. https://doi.org/10.5194/bg-10-6247-2013

Porter, C., Morin, P., Howat, I., Noh, M.-J., Bates, B., Peterman, K., et al. (2018). ArcticDEM. https://doi.org/10.7910/DVN/OHHUKH

R Core Team. (2018). *R: A language and environment for statistical computing*. R Foundation for Statistical Computing. Retrieved from http://www.r-project.org/

Reyes, F. R., & Lougheed, V. L. (2015). Rapid nutrient release from permafrost thaw in arctic aquatic ecosystems. *Arctic Antarctic and Alpine Research*, *47*(1), 35–48. https://doi.org/10.1657/AAAR0013-099

Robinne, F.-N., Hallema, D. W., Bladon, K. D., & Buttle, J. M. (2020). Wildfire impacts on hydrologic ecosystem services in north American high-latitude forests: A scoping review. *Journal of Hydrology*, *581*, 124360. https://doi.org/10.1016/j.jhydrol.2019.124360

Rocha, A. V., Loranty, M. M., Higuera, P. E., Mack, M. C., Hu, F. S., Jones, B. M., et al. (2012). The footprint of Alaskan tundra fires during the past half-century: Implications for surface properties and radiative forcing. *Environmental Research Letters*, *7*(4), 044039. https://doi.org/10.1088/1748-9326/7/4/044039

Rodríguez-Cardona, B. M., Coble, A. A., Wymore, A. S., Kolosov, R., Podgorski, D. C., Zito, P., et al. (2020). Wildfires lead to decreased carbon and increased nitrogen concentrations in upland arctic streams. *Scientific Reports*, *10*(1), 8722. https://doi.org/10.1038/s41598-020-65520-0

Sae-Lim, J., Russell, J. M., Vachula, R. S., Holmes, R. M., Mann, P. J., Schade, J. D., & Natali, S. M. (2019). Temperature-controlled tundra fire severity and frequency during the last millennium in the Yukon-Kuskokwim Delta, Alaska. *The Holocene*, *29*(7), 1233. https://doi.org/10.1177/0959683619838036

Shogren, A. J., Zarnetske, J. P., Abbott, B. W., Iannucci, F., Frei, R. J., Griffin, N. A., & Bowden, W. B. (2019). Revealing biogeochemical signatures of Arctic landscapes with river chemistry. *Scientific Reports*, *9*(1), 12894. https://doi.org/10.1038/s41598-019-49296-6

Stanley, E. H., Casson, N. J., Christel, S. T., Crawford, J. T., Loken, L. C., & Oliver, S. K. (2016). The ecology of methane in streams and rivers: Patterns, controls, and global significance. *Ecological Monographs*, *86*(2), 26. https://doi.org/10.1890/15-1027.1

Striegl, R. G., Dornblaser, M. M., Aiken, G. R., Wickland, K. P., & Raymond, P. A. (2007). Carbon export and cycling by the Yukon, Tanana, and porcupine rivers, Alaska, 2001-2005. *Water Resources Research*, *43*(2), 1–9. https://doi.org/10.1029/2006WR005201

Stubbins, A., Silva, L. M., Dittmar, T., & Van Stan, J. T. (2017). Molecular and optical properties of tree-derived dissolved organic matter in throughfall and stemflow from live oaks and eastern red cedar. *Frontiers of Earth Science*, *5*, 22. https://doi.org/10.3389/feart.2017.00022

Tondu, J. M. E., Turner, K. W., Wolfe, B. B., Hall, R. I., Edwards, T. W. D., & McDonald, I. (2013). Using water isotope tracers to develop the hydrological component of a long-term aquatic ecosystem monitoring program for a northern lake-rich landscape. *Arctic Antarctic and Alpine Research*, *45*(4), 594–614. https://doi.org/10.1657/1938-4246-45.4.594

Toohey, R. C., Herman-Mercer, N. M., Schuster, P. F., Mutter, E. A., & Koch, J. C. (2016). Multidecadal increases in the Yukon River Basin of chemical fluxes as indicators of changing flowpaths, groundwater, and permafrost. *Geophysical Research Letters*, *43*(23), 12120–12130. https://doi.org/10.1002/2016GL070817

Tozer, B., Sandwell, D. T., Smith, W. H. F., Olson, C., Beale, J. R., & Wessel, P. (2019). Global bathymetry and topography at 15 arc sec: SRTM15+. *Earth and Space Science*, *6*(10), 1847–1864. https://doi.org/10.1029/2019EA000658

Turner, K. W., Edwards, T. W. D., & Wolfe, B. B. (2014). Characterising runoff generation processes in a lake-rich thermokarst landscape (Old Crow Flats, Yukon, Canada) using $\delta^{18}O$, $\delta^{2}H$ and d-excess measurements. *Permafrost and Periglacial Processes*, *25*(1), 53–59. https://doi.org/10.1002/ppp.1802

U.S. Environmental Protection Agency. (1984). Methods for chemical analysis of water and wastes. No. EPA-600/4-79-020.

Veraverbeke, S., Rogers, B. M., Goulden, M. L., Jandt, R. R., Miller, C. E., Wiggins, E. B., & Randerson, J. T. (2017). Lightning as a major driver of recent large fire years in North American boreal forests. *Nature Climate Change*, *7*(7), 529–534. https://doi.org/10.1038/nclimate3329

Wang, L., & Liu, H. (2006). An efficient method for identifying and filling surface depressions in digital elevation models for hydrologic analysis and modelling. *International Journal of Geographical Information Science*, *20*(2), 193–213. https://doi.org/10.1080/13658810500433453

Ward, C. P., & Cory, R. M. (2016). Complete and partial photo-oxidation of dissolved organic matter draining permafrost soils. *Environmental Science & Technology*, *50*(7), 3545–3553. https://doi.org/10.1021/acs.est.5b05354

Weishaar, J. L., Aiken, G. R., Bergamaschi, B. A., Fram, M. S., Fujii, R., & Mopper, K. (2003). Evaluation of specific ultraviolet absorbance as an indicator of the chemical composition and reactivity of dissolved organic carbon. *Environmental Science & Technology*, *37*(20), 4702–4708. https://doi.org/10.1021/es030360x

Wessel, P., Luis, J. F., Uieda, L., Scharroo, R., Wobbe, F., Smith, W. H. F., & Tian, D. (2019). The generic mapping tools version 6. *Geochemistry, Geophysics, Geosystems*, *20*(11), 5556–5564. https://doi.org/10.1029/2019GC008515

Wheeler, B., & Torchiano, M. (2016). Package lmPerm (version 2.1.0). Retrieved from https://cran.r-project.org/web/packages/lmPerm/index.html

Wickland, K. P., Aiken, G. R., Butler, K., Dornblaser, M. M., Spencer, R. G. M., & Striegl, R. G. (2012). Biodegradability of dissolved organic carbon in the Yukon River and its tributaries: Seasonality and importance of inorganic nitrogen. *Global Biogeochemical Cycles*, *26*(4), 1–14. https://doi.org/10.1029/2012GB004342

Young, A. M., Higuera, P. E., Duffy, P. A., & Hu, F. S. (2017). Climatic thresholds shape northern high-latitude fire regimes and imply vulnerability to future climate change. *Ecography*, *40*(5), 606–617. https://doi.org/10.1111/ecog.02205

Yue, X., Mickley, L. J., Logan, J. A., Hudman, R. C., Martin, M. V., & Yantosca, R. M. (2015). Impact of 2050 climate change on North American wildfire: Consequences for ozone air quality. *Atmospheric Chemistry and Physics*, *15*(17), 10033–10055. https://doi.org/10.5194/acp-15-10033-2015

Zolkos, S., MacDonald, E., Hung, J., Schade, J., Ludwig, S., Mann, P., et al. (2022). *Wildfire effects on aquatic chemistry (Yukon Kuskokwim delta, Alaska), 2015-2019*. NSF Arctic Data Center. https://doi.org/10.18739/A2K35MF90